Optics Letters

Ultrabroadband mid-infrared noncollinear difference frequency generation in a silver thiogallate crystal

Yaroslav V. Aulin,[1,†] Aashish Tuladhar,[1,2,†] and Eric Borguet[1,*]

[1]Department of Chemistry, Temple University, 1901 N. 13th Street, Philadelphia, Pennsylvania 19122, USA
[2]Physical & Computational Sciences Directorate, Pacific Northwest National Laboratory, Richland, Washington 99352, USA
*Corresponding author: eborguet@temple.edu

Received 15 May 2018; revised 17 July 2018; accepted 9 August 2018; posted 9 August 2018 (Doc. ID 331419); published 11 September 2018

We report the generation of ultrabroadband mid-infrared (mid-IR) pulses by noncollinear difference frequency mixing. The signal and the idler output beams of an optical parametric amplifier are combined in a silver thiogallate crystal ($AgGaS_2$) to generate mid-infrared radiation. We show that a noncollinear geometry facilitates broadband phase matching. Spectral bandwidths up to 1750 cm^{-1} were obtained at an external noncollinear angle of 4.2 deg, which is more than three times broader than in a collinear geometry. The broadband spectrum is tunable in the range of 1500–4500 cm^{-1}. Pulse energies up to 1 μJ were achieved. The broadband pulses were used in sum frequency generation in ZnSe and in vibrational absorption spectroscopy experiments of liquid samples. © 2018 Optical Society of America

OCIS codes: (190.4360) Nonlinear optics, devices; (190.7110) Ultrafast nonlinear optics; (190.4223) Nonlinear wave mixing; (140.7090) Ultrafast lasers.

https://doi.org/10.1364/OL.43.004402

The mid-infrared (mid-IR) spectral range (400–4000 cm^{-1}) covers the fundamental vibrational transitions of many molecules and solid-state compounds [1–3]. Due to this, it is extremely important for various fields such as vibrational spectroscopy [4], chemical identification (fingerprint region) [3], and remote sensing [5] to develop ultrafast broadband mid-IR sources. Ultrafast vibrational spectroscopy techniques such as surface selective sum frequency generation spectroscopy or two dimensional and multi-dimensional vibrational spectroscopies will especially benefit from ultrafast broadband mid-IR sources.

There are a few different techniques that could be used to generate mid-IR radiation: quantum cascade lasers [6], optical parametric amplification, optical parametric oscillators [7], supercontinuum generation [4,8], and difference frequency generation (DFG) [9]. The advantage of the DFG approach is a broad tuning range over the mid-IR spectrum [10]. Tuning is typically performed by rotation of the nonlinear crystal and proper selection of polarizations, wavelengths, and bandwidths of the input pump and the seed laser sources.

Similar to optical parametric amplification [11], DFG allows for broadband phase matching in a noncollinear geometry [12]. Noncollinear DFG in an AGS ($AgGaS_2$—silver thiogallate) crystal was first used by Lahman *et al.* to generate tunable infrared output using continuous-wave lasers [13]. Haidar *et al.* [14] demonstrated tunable narrow band DFG of mid-IR pulses by mixing the signal and the idler output of an optical parametric oscillator in an AGS crystal. DFG with femtosecond pulses in a noncollinear geometry was studied by Rotermund and Petrov in an AGS crystal pumped at 1250 nm, resulting in a bandwidth of up to 265 nm (73 cm^{-1}) at 6 μm [15]. Sugita *et al.* further expanded this research by theoretically and experimentally studying broadband phase matching in a noncollinear geometry in AGS [12] for pump and seed laser pulses centered at 760 and 800 nm. It was shown that type I, rather than type II, phase matching is responsible for broadband generation. The noncollinear phase matching extended the bandwidth by a factor of 5 up to 300 cm^{-1}. However, this is not enough in many fields of study where ultrabroadband IR is needed: for instance, the generation of attosecond pulses, high-harmonic generation, extreme ultraviolet and soft X-ray generation, and coherent control of chemical reactions [16,17].

Recent research in the field of noncollinear DFG of mid-IR sources was mostly focused on the exploration of novel and more efficient nonlinear materials such as $CdSiP_2$ [18], rather than increasing the mid-IR bandwidth. The bandwidth of the mid-IR sources has been vastly improved (~4000 cm^{-1}) by using supercontinuum generation in chalcogenide glasses [4]. However, this approach has a number of limitations such as instability, low power conversion efficiency, spatial chirp, and fragility of glasses. In this Letter, we use noncollinear phase matching towards the generation of easily tunable, ultrabroadband radiation by difference frequency mixing of the near-infrared signal and idler output of an optical parametric amplifier (OPA) in an AGS crystal. By employing a simple design of separating and recombining the signal and idler beam (without the need for any focusing optics) in a slightly noncollinear

angle, we propose that any commercial DFG laser can be modified to generate more mid-IR bandwidth.

The experimental setup used to study noncollinear DFG (Fig. 1) employs a one box Ti:sapphire oscillator and regenerative amplifier (Coherent Libra) to produce 5 mJ, 100 fs pulses at 800 nm with a 1 kHz repetition rate. 90% of the Libra output was used to pump a Light Conversion TOPAS Prime OPA producing 1.3 W signal+idler output, while 10% was used to produce spectrally narrowed (~2 nm, pulse duration ~1 ps) 800 nm pulses using a narrow bandpass filter (CVI Laser Optics) for sum frequency characterization of the mid-IR output. The signal and idler output beams of the OPA, which were spatially separated by a dichroic beam splitter, were spatially and temporarily overlapped in the 1 mm thick 8×8 mm^2 AGS crystal cut at angles $\theta = 51°$ $\varphi = 45°$ (Eksma Optics). The crystal was coated with broadband antireflective coatings for the optical ranges of 1.1–2.6 μm and 2.6–11.0 μm.

Silver thiogallate ($AgGaS_2$) is a nonlinear negative uniaxial crystal [19,20] with a wide transparency range (from 500 nm to 13.2 μm) [21,22]. This means that the phase matching could be achieved in a type I implementation [23]. In our configuration, the OPA idler wave is o (ordinary), i.e., polarized perpendicular to the optical axis of the AGS crystal, and the OPA signal wave is e (extraordinary), i.e., polarized in the plane formed by the optical axis and the propagation vector. The type I interaction results in an ordinary polarized difference frequency wave in the AGS crystal. A delay stage was introduced in the idler beam to control the temporal overlap between the signal and the idler beams. No focusing elements were used in the signal or the idler beam to keep the fluence (40 GW/cm^2) below the damage threshold of the AGS crystal [15] (200 GW/cm^2) and to maintain the beam profile (collimation). The diameters of the signal and idler beams were measured to be 5 mm (90% intensity). The orientation of the crystal was adjusted to achieve broadband phase matching.

The residual signal and idler beams were filtered out from the mid-IR light using a 2600 nm long-pass filter (Edmund Optics). The DFG beam was circularly shaped, as determined by the spot on a thermal detector card. The shape of the beam was not affected by the noncollinear geometry. To characterize the spectrum, the mid-IR beam was focused onto a 1 mm thick polycrystalline ZnSe plate (Meller Optics). The spectrally narrowed 800 nm pulse was spatially and temporarily overlapped onto the ZnSe plate with the mid-IR pulse, generating sum frequency photons. The residual scattered 800 nm beam was filtered out from the sum frequency pulse by a 750 nm short-pass filter (Melles Griot) and coupled into an optical fiber connected to an Acton SpectraPro-300i imaging spectrograph equipped with a Princeton Instruments charge-coupled device (CCD LN/100B) cooled down to −120°C using liquid nitrogen.

We performed the theoretical analysis of the DFG in an AGS crystal using the SNLO software package [23]. The mid-IR pulse is created by a DFG process between the signal and idler waves. The energy conservation condition can be written as

$$h\nu_{\text{midIR}} = h\nu_S - h\nu_I. \quad \textbf{(1)}$$

Phase matching between signal, idler, and DFG waves propagating in the crystal is critical for efficient difference frequency mixing of the photons.

The phase-matching condition can be written using the following expression:

$$\Delta\vec{k} = \vec{k}_S - \vec{k}_I - \vec{k}_{\text{DFG}} = 0, \quad \textbf{(2)}$$

where Δk is the phase mismatch, and k_S, k_I, and k_{DFG} are the wave vectors of the signal, idler, and DFG waves, respectively.

A phase-matching curve determines which wavelength of mid-IR radiation can be efficiently generated for a certain noncollinear angle α for the OPA idler wave propagating at the angle θ with respect to an optical axis of the crystal (Fig. 2).

The vertical regions of the phase-matching curve, i.e., where the DFG wavenumber does not depend on θ, correspond to the broadband phase-matching case. In such vertical regions, multiple wavelengths of signal and idler waves propagating in the same direction could be simultaneously phase matched and lead to broadband mid-IR difference frequency output.

Phase-matching curves were generated for different signal wavelengths in the range 1200–1400 nm for internal noncollinear angles between the OPA signal and idler waves ranging from 0° to 6°. In general, noncollinear geometry allows for broadband phase matching. This can be seen by comparing $\alpha = 0°$ and $\alpha = 2.5°$ in Fig. 3. The broadest phase matching is predicted for the 1300 nm signal wavelength interacting with the idler wave with wavelengths in the range of 1670–2700 nm

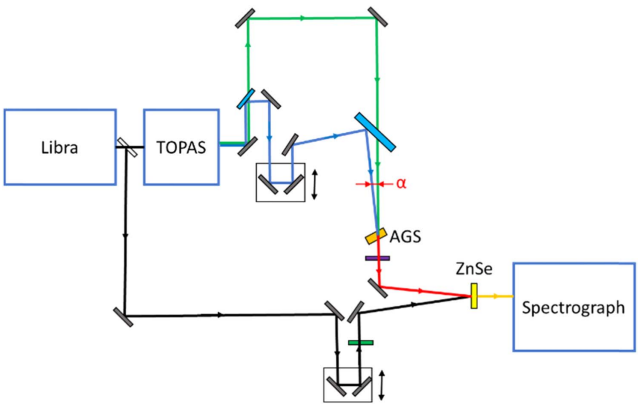

Fig. 1. Experimental setup used in noncollinear DFG generation experiments. Black, 800 nm beam; green, idler; blue, signal; red, mid-IR; orange, sum frequency of mid-IR and 800 nm.

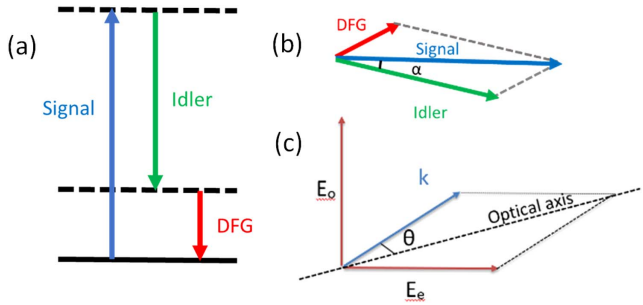

Fig. 2. Energy diagram of the DFG process. (a) Signal and idler photons interact in a nonlinear crystal to produce the difference frequency photons. (b) Momentum conservation vector diagram in noncollinear geometry (α—internal noncollinear angle between the signal and idler wave vectors). (c) Polarizations of ordinary and extraordinary waves in a uniaxial crystal.

(3700–6000 cm^{-1}) because the phase-matching curve is vertical at $\theta = 43°$ over the widest range (2000–4000 cm^{-1}) for the internal noncollinear angle of 2.5° (4.2° external angle in our configuration). The range of mid-IR difference frequency wavelengths generated is 2500–5890 nm (1700–4000 cm^{-1}).

The calculations performed for different pump wavelengths in the range of 1200–1400 nm show broadband phase matching for internal noncollinear angles 2–3°. The broadband phase-matching angle shifts from 46° for 1200 nm to 39° for 1400 nm.

The bandwidth of mid-IR radiation increased from 500 cm^{-1} in a collinear geometry to 1750 cm^{-1} for a noncollinear angle of 4.2° (Fig. 4). The spectral bandwidth was measured at the 10% power level. At the same time, we observed the decrease of the mid-IR pulse energy from 10 μJ in collinear geometry to a pulse energy of 1 μJ at external noncollinear angle of 4.2°.

The tuning of the mid-IR output spectrum was achieved by changing the TOPAS OPA output wavelengths. The mid-IR spectra obtained for different pump wavelengths in the range of 1200–1400 nm are shown in Fig. 5.

The broadband radiation produced by DFG in silver thiogallate was used to measure the absorption spectra of various liquids such as water, methanol, and ethanol. The liquid sample trapped between two microscope slides was placed into the mid-IR beam path. Two empty glass slides were also placed into an 800 nm visible beam path to achieve temporal overlap. The change in the mid-IR spectrum was monitored, and the optical density was calculated as shown in Fig. 6. The spectrum covers the range of 2000–4000 cm^{-1}. The bandwidth of the source covers both OH and OD stretch spectral ranges. This suggests that the radiation produced by the source can be used for spectroscopy of H_2O/D_2O mixtures in sum frequency generation spectroscopy of aqueous interfaces [24,25].

Our results on spectral broadening during the DFG process in a noncollinear geometry compared to a collinear geometry are consistent with the results of Sugita *et al.* [12] on broadband mid-IR generation (230 cm^{-1} bandwidth), who employed the output of a Ti:sapphire oscillator to produce pump and seed pulses centered at 800 nm and used them for DFG in AGS

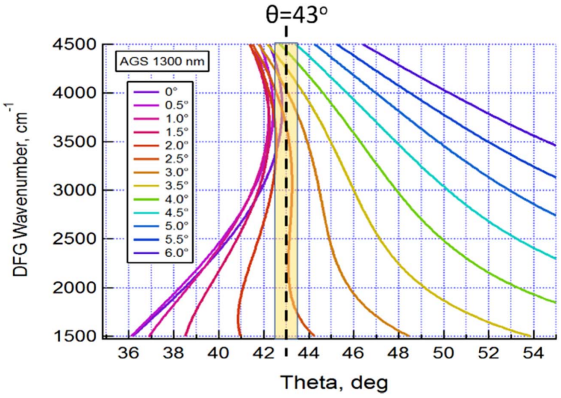

Fig. 3. Phase-matching curves for type I phase matching in an AGS crystal for a pump wavelength of 1300 nm at different noncollinear angles (α). Broadband phase matching is achieved for $\alpha = 2.5°$ and $\theta = 43°$. The highlighted region corresponds to the range of phase-matching angles $\theta = 43° \pm 0.5°$.

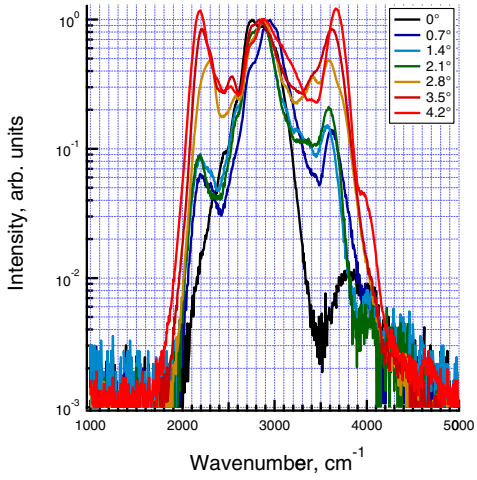

Fig. 4. Mid-IR spectra determined by sum frequency (DFG output +800 nm pulse) for different external noncollinear angles, TOPAS signal wavelength of 1300 nm.

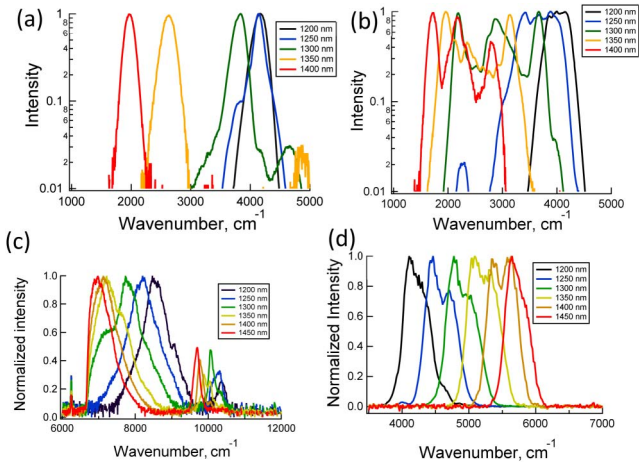

Fig. 5. Tunability of the mid-IR output achieved by changing the OPA signal wavelength for (a) collinear and (b) noncollinear (4.2° external noncollinear angle, corresponding to 1.7° internal noncollinear angle) geometries, spectra of (c) the signal and (d) the idler output of the OPA.

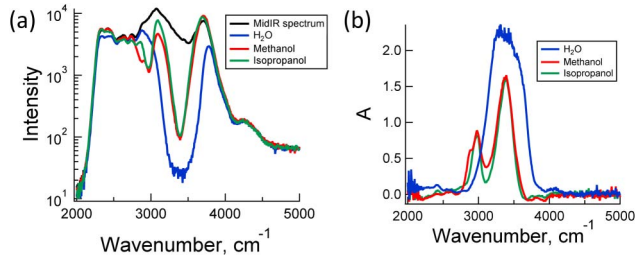

Fig. 6. Mid IR absorption spectra of water, methanol, and ethanol acquired with a broadband DFG source: (a) spectra of mid-IR radiation transmitted through the samples and (b) optical density of the samples in the mid-IR spectral range calculated using the Beer–Lambert law.

to obtain mid-IR radiation in the 850–1100 cm^{-1} spectral range. We have expanded this approach to the 1500–4000 cm^{-1} spectral range and demonstrated the use of the signal and idler output of a commercial OPA source. We achieved almost 10 times improvement in bandwidth compared to the results of Sugita *et al.* The mid-IR spectral bandwidths obtained in our research are narrower than recently reported bandwidths of mid-IR spectra generated using other methods such as supercontinua, where mid-IR pulses of up to 4000 cm^{-1} bandwidth were obtained in chalcogenide glasses by Petersen *et al.* [4]. The drawback of the continuum generation technique is that the mid-IR source generated is unstable, and the chalcogenide glasses are fragile. It has no scale-up possibility due to its inherent instability that comes from the brittle nature of the glass which leads to optical damage to the material. In addition, a beam focusing geometry is already employed to reach the intensities required for continuum generation. In contrast, our method uses nonlinear crystals that are already exploited in commercial OPAs due to their durability and demonstrated generation of stable mid-IR output. In addition, since no focusing optics is employed in the current design, this approach provides us with a scope for power scale-up. By increasing both signal and idler fluence by the factor of 5, we expect a 25-fold increase in mid-IR power. The spectrum and the power of our mid-IR source were stable during at least five hours, with any instabilities arising from the fluctuations in the regenerative amplifier and OPA output, rather than thermal effects or damage of the AGS crystal.

In summary, we employed a noncollinear geometry to expand the bandwidth of mid-IR light produced from a commercial OPA by DFG. We showed that ultrabroadband mid-IR output with a bandwidth up to 1750 cm^{-1} (at 10% power level) can be generated in a silver thiogallate (AGS) crystal for an internal noncollinear angle between signal and idler waves of approximately 2°. We characterized the mid-IR spectrum by sum frequency generation in a ZnSe crystal and performed the mid-IR absorption spectroscopy of liquid samples. The generation of mid-IR broadband by noncollinear DFG has a number of advantages over other methods reported in literature (filamentation, supercontinuum generation) such as stability and potential for scaling up in power.

Funding. National Science Foundation (NSF) (CHE 1337880).

Acknowledgment. A. T. acknowledges support by the US Department of Energy (DOE), Office of Basic Energy Sciences, Division of Materials Science and Engineering at Pacific Northwest National Laboratory (PNNL).

[†]These authors contributed equally to this Letter.

REFERENCES

1. I. T. Sorokina and K. L. Vodopyanov, *Solid-state Mid-Infrared Laser Sources* (Springer-Verlag, 2003).
2. J. Biegert, O. Chalus, and P. Bates, *Coherence and Ultrashort Pulse Laser Emission* (Intech Open, 2010).
3. A. Sugiharto, C. M. Johnson, H. De Aguiar, L. Alloatti, and S. Roke, Appl. Phys. B **91**, 315 (2008).
4. A. M. Stingel, H. Vanselous, and P. B. Petersen, J. Opt. Soc. Am. B **34**, 1163 (2017).
5. J. D. Suter, B. E. Bernacki, and M. C. Phillips, Proc. SPIE **8268**, 826801 (2012).
6. Y. Yao, A. J. Hoffman, and C. F. Gmachl, Nat. Photonics **6**, 432 (2012).
7. V. V. Badikov, P. Blinov, A. Kosterev, V. S. Letokhov, A. L. Malinovsky, and E. A. Ryabov, Quantum Electron. **27**, 523 (1997).
8. P. B. Petersen and A. Tokmakoff, Opt. Lett. **35**, 1962 (2010).
9. R. W. Boyd, *Nonlinear Optics* (Academic Press, 2003).
10. L. Wang, Z. Cao, H. Wang, H. Zhao, W. Gao, Y. Yuan, W. Chen, W. Zhang, Y. Wang, and X. Gao, Opt. Commun. **284**, 358 (2011).
11. O. Isaienko and E. Borguet, Opt. Express **16**, 3949 (2008).
12. A. Sugita, K. Yokoyama, H. Yamada, N. Inoue, M. Aoyama, and K. Yamakawa, Jpn. J. Appl. Phys. **46**, 226 (2007).
13. W. Lahmann, K. Tibulski, and H. Welling, Opt. Commun. **17**, 18 (1976).
14. S. Haidar, K. Nakamura, E. Niwa, K. Masumoto, and H. Ito, Appl. Opt. **38**, 1798 (1999).
15. F. Rotermund and V. Petrov, Jpn. J. Appl. Phys. **40**, 3195 (2001).
16. T. Popmintchev, M. C. Chen, D. Popmintchev, P. Arpin, S. Brown, S. Ališauskas, G. Andriukaitis, T. Balčiunas, O. D. Mücke, and A. Pugzlys, Science **336**, 1287 (2012).
17. H. Liang, P. Krogen, Z. Wang, H. Park, T. Kroh, K. Zawilski, P. Schunemann, J. Moses, L. F. DiMauro, and F. X. Kärtner, Nat. Commun. **8**, 141 (2017).
18. D. Sánchez, M. Hemmer, M. Baudisch, K. Zawilski, P. Schunemann, H. Hoogland, R. Holzwarth, and J. Biegert, J. Opt. Lett. **39**, 6883 (2014).
19. D. Chemla, P. Kupecek, D. Robertson, and R. Smith, Opt. Commun. **3**, 29 (1971).
20. G. Boyd, H. Kasper, and J. McFee, IEEE J. Quantum Electron. **7**, 563 (1971).
21. G. Bhar and R. Smith, Phys. Status Solidi A **13**, 157 (1972).
22. U. Willer, T. Blanke, and W. Schade, Appl. Opt. **40**, 5439 (2001).
23. A. V. Smith, *Crystal Nonlinear Optics: with SNLO Examples* (AS-Photonics, 2015).
24. A. Tuladhar, S. M. Piontek, L. Frazer, and E. Borguet, J. Phys. Chem. C **122**, 12819 (2018).
25. A. Tuladhar, S. M. Piontek, and E. Borguet, J. Phys. Chem. C **121**, 5168 (2017).